Research Article | Vol. 12, No. 9 / 1 Sep 2021 / Biomedical Optics Express 5844
Biomedical Optics EXPRESS

Photopolymerization strategy for the preparation of small-diameter artificial blood vessels with micro-nano structures on the inner wall

YONGHAO LIU,[1,3] JIAWEI ZHANG,[2] SHUNXIN LI,[2,4] AND HONG XIA[2,5]

[1]*Heilongjiang Provincial Key Laboratory of Oilfield Applied Chemistry and Technology, School of Mechatronics Engineering, Daqing Normal University, Daqing 163712, China*
[2]*State Key Laboratory of Integrated Optoelectronics, College of Electronic Science and Engineering, Jilin University, Changchun 130012, China*
[3]*yonghaoliu1980@163.com*
[4]*shunxin2021@jlu.edu.cn*
[5]*hxia@jlu.edu.cn*

Abstract: Although large diameter vessels made of polyurethane materials have been widely used in clinical practice, the biocompatibility and long-term patency of small diameter artificial vessels have not been well addressed. Any technological innovation and advancement in small-diameter artificial blood vessels is of great interest to the biomedical field. Here a novel technique is used to produce artificial blood vessels with a caliber of less than 6 mm and a wall thickness of less than 0.5 mm by rotational exposure, and to form a bionic inner wall with a periodically micro-nano structure inside the tube by laser double-beam interference. The polyethylene glycol diacrylate used is a widely recognized versatile biomaterial with good hydrophilicity, biocompatibility and low cytotoxicity. The effect of the bionic structure on the growth of hepatocellular carcinoma cells and human umbilical vein endothelial cells was investigated, and it was demonstrated that the prepared vessels with the bionic structure could largely promote the endothelialization process of the cells inside them.

1. Introduction

In the last two decades, with the development of human technology and the improvement of living standards, cardiovascular and cerebrovascular diseases have become the number one killer among human diseases worldwide, among which the occlusive diseases, mainly atherosclerosis, are the most representative. [1]. The most effective treatment for these diseases is the timely replacement of blood vessels, [2,3] and the limited availability of autologous blood vessels and homologous vessels has led to the widespread clinical use of artificial blood vessels, of which medium and large caliber artificial blood vessels prepared from polyurethane materials have been commercialized. However, for small-diameter (< 6 mm) artificial vessels, the vessels prepared by existing processes suffer from serious problems such as poor anticoagulation ability and poor long-term patency [4,5]. Since the polymer artificial blood vessels prepared by spinning and other means do not have an internal microstructure or the structure is too simple, resulting in the inability to grow a continuous layer of endothelial cells on the internal surface of the implanted blood vessels in a short period of time, they can induce platelet adsorption to produce thrombus and then vascular obstruction and other problems [6–9]. Domestic and international research has been focused on the bionic processing of artificial vascular microstructures, and most studies have shown that the bionic microstructures have led to a significant improvement in the biocompatibility of polymeric materials [10–14]. Professor Seifalian, a famous British

#432441 https://doi.org/10.1364/BOE.432441
Journal © 2021 Received 8 Jul 2021; revised 15 Aug 2021; accepted 16 Aug 2021; published 26 Aug 2021

Biomedical Optics EXPRESS

nanotechnology and tissue repair scientist, pointed out that micro-nano-structured processing is the main direction for the future development of artificial small-diameter blood vessels [7].

In tissue engineering polyethylene glycol (PEG) hydrogel systems have a wide research value and their wide range and excellence of mechanical and biological properties leding to their use in multiple biomedical fields including drug carriers, tissue engineering scaffolds, and wound dressings [15–18]. Acrylate-derived PEG (PEGDA) can be cross-linked and maintain good biocompatibility under mild conditions, and such materials have high permeability and high water-content [19–22]. When the molecular weight and concentration of PEGDA change, a series of matrix modulus and swelling ratio changes are similar to many soft tissues [23]. In addition, PEG hydrogels can resist protein-cell adhesion on their surface, thus serving as a biological template to reduce immune responses, as well as the ability to modify biological properties by adjusting surface physicochemical properties [24]. The chemical properties of PEG glycols can be readily adjusted in a controlled manner by altering surface functional groups. It is also possible to modulate its degradation time in the organism, which can lead to rapid degradation or long-term stabilization of the carrier [25].

Optical processing technology is of great interest to the processing field for its convenience, speed and other advantages [2627]. Since its application, laser has been highly valued by the research field because of a series of advantages such as good directionality, high energy and monochromaticity [28–30]. Laser processing technology has driven the rapid development of many fields and has an increasingly wide range of applications [31–33]. In order to solve the problems faced by the above-mentioned traditional small-diameter blood vessel fabrication methods, in this paper we use a new small-diameter blood vessel preparation technique, the rapid rotational exposure photopolymerization method. The UV light is focused in a rotatable cylinder mold that can be rotated to transmit wavelength light and is filled with a pre-polymerization solution. Here we have chosen a biologically sound PEGDA with the photoinitiator 2-hydroxy-2-methylpropiophenone (Daracure 1173) as the pre-polymerization solution, which is rotated through the mold and processed by UV-curable pre-polymerization system in the axial direction until the thickness reaches a specified value. Afterwards, the micro-nano structure is processed by laser double-beam interference on the inner wall of the formed vascular precursors. Multi-beam interference processing is cost-effective, suitable for batch processing and production, and is highly accurate, with nanowires with feature sizes of 100 nm being commonly achieved [34–37]. Most importantly, high-precision, multi-layered, and complex micro-nano structures can be prepared using multi-beam laser interference methods [38–42]. For example, Saulius Juodkazis and coworkers had achieved biomimetic hierarchical 3D textures by multi-beam interference lithography [42]. Most of the failures of coronary stents with small diameter vessels are due to thrombosis and the risk of bleeding when adjuvant intervention is performed with antiplatelet drugs [4344]. Therefore, we wanted the prepared small-diameter artificial vessels to complete the endothelialization process rapidly and thus significantly improve their long-term patency in vivo. We cultured hepatocellular carcinoma cells (hcc) with human umbilical vein endothelial cells (huvec) on the inner walls of the blood vessels with micro-nano structure and found experimentally that the use of the micro-nano structures processed by the intervention significantly increased the number of endothelial cell adhesions and had an effect on the arrangement of cells on the inner wall. Artificial blood vessels should have more complex structures rather than simple tubular structures for practical application, and many researchers have made great progress in this field [4546]. For example, 3D patterns of biocompatible and cross-linkable materials serve as cellular scaffolds have been successfully achieved by direct laser writing [47]. However, our preparation method of this simple tubular structure can be used as the research basis for further developing more complex artificial blood vessel structures in the future.

Biomedical Optics EXPRESS

2. Results and discussion

2.1. Fabrication of the small diameter vascular prosthesis with a micro-nano structure by rotary exposure

The schematic diagram of the turntable model for rapid processing of blood vessels was shown in Fig. 1(a). In order to obtain the artificial blood vessels with adjustable wall thickness, we use the technology of turntable exposure and cannula to process. We use two glass tubes with different radii to cover the large tube on the outside of the small tube, and wrap a rubber ring at the bottom of the small tube to make the distance between the circumference and the large tube equal. The photo of used equipment was shown in Fig. S1. In the gap, we can add the pre-exposure solution and complete circular exposure by spinning. The thickness of the inner wall of the vessel was the inner diameter of the outer tube and the outer diameter of the inner tube, and the radius of the vessel was the outer diameter of the inner tube. Through the rotation of the motor to drive the rotation of the cannula, the artificial blood vessel was quickly and evenly solidified from pre-exposure solution through UV exposure. In this process, a UV lamp with nonadjustable power and large spot is used. Therefore, we control the exposure dose by controlling the distance between the sample and the UV light source, exposure time and exposure speed. Through experiments, we found that when the exposure distance is too close, the obtained artificial blood vessel will undergo unexpected deformation due to the thermal effect of UV lamp, because the power of UV lamp cannot be regulated, so it is necessary to find an appropriate exposure position. When the distance increases, the exposure time needs to increase accordingly, and when the exposure distance exceeds the critical value, no matter how to increase the exposure time, the polymerization of pre-exposure solution cannot be completed. The increase of rotating speed can reduce the single point exposure time and alleviate the thermal effect caused by distance. Based on the above three points, we found the optimal exposure parameters: the rotating speed is 240 rpm, the exposure time is 5 min and the exposure distance is 10 cm. The power density of UV light is about 6.5 $mW\mu m^{-2}$. Under these parameters, the solution can complete the exposure in a short time, and the mechanical properties of the vascular precursors are intact without overheating deformation. The insert of Fig. 1(b) shows the acquired primarily uniform and transparent vessel with an internal diameter of 5 mm. As shown in the SEM images of the prepared blood vessel (Fig. S2), the thickness of the tube wall is about 500 μm. And the inner surface structure is smooth, which can be used to realize further micro-nano structure processing.

Because the artificial blood vessel not only needs good biological properties, but also its mechanical properties in vivo are very important, we characterized the tensile strength of the artificial vessel. The maximum uniform plastic deformation resistance of the vessel was tested. A uniform external tensile force was implemented to the blood vessel, resulting in uniform deformation of the vessel. With the increase of the force, the fracture surface appears in the vessel, and the tensile force per unit area is the tensile strength of the vessel. Its expression is $\sigma_b = F_b/S_0$ (MPa), σ_b is tensile strength, its unit is MPa, F_b is the maximum tensile force (N) of the sample, and S_0 is the original cross-sectional area of the ring. The re-exposure solution is mainly composed of PEGDA and water. Adjusting the ratio of PEGDA and water can obtain excellent mechanical properties. When the ratio is 1:1.7 the vessel has the best mechanical properties, The test results are shown in Fig. 1(b). The maximum tensile strength of the prepared vessels is 0.60 MPa and that of commercial vessels is above 0.65 MPa. It can be seen that the synthetic vessels basically meet the requirements. The effect of exposure time on wall thickness and maximum bearing pressure is shown in Table S1. The appropriate water content is also important for the morphology of the inner wall of vessels. When the water content is high, the inner wall ranges rise and fall after dehydration and drying greatly, and the morphology presents two levels of roughness (Fig. S3). The first level mainly shows a large range of fluctuation, and the second level morphology is mainly characterized by densely distributed folds on the surface,

Biomedical Optics EXPRESS

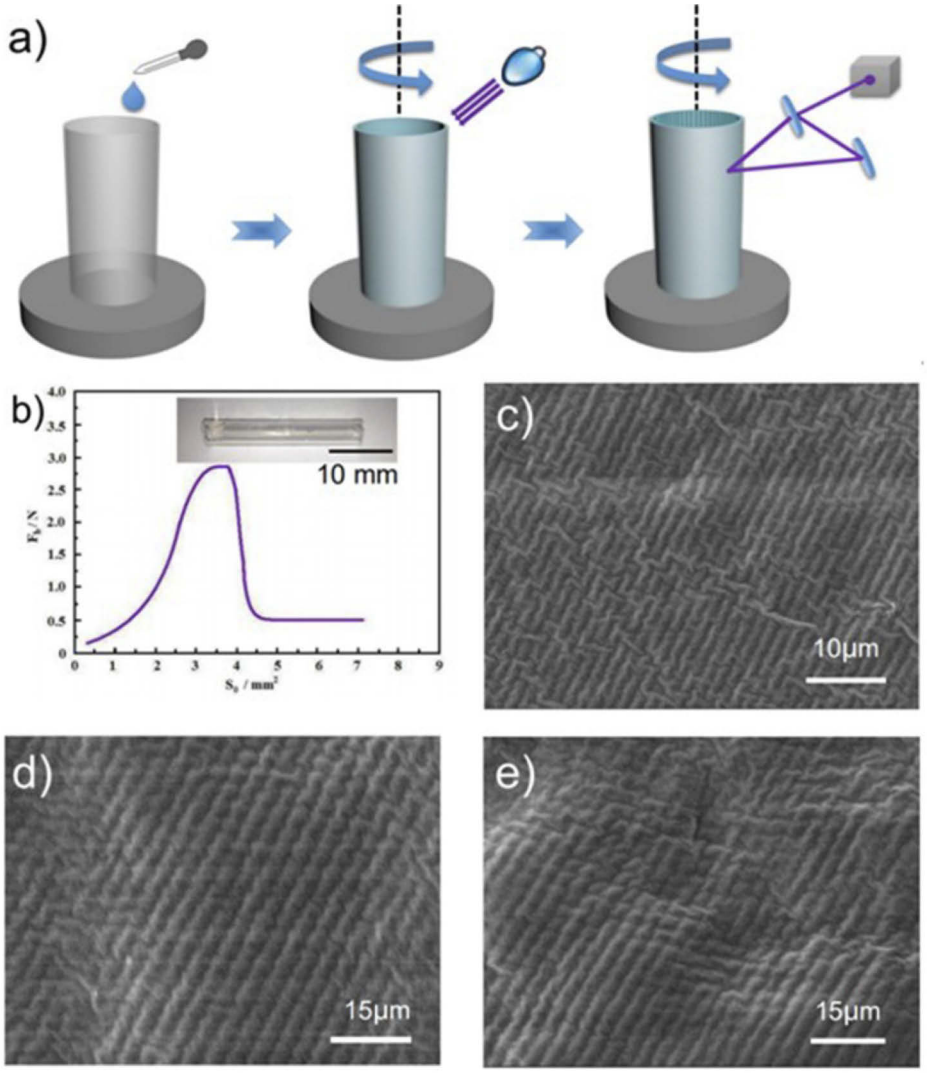

Fig. 1. (A) Scheme of preparation of the small diameter blood vessel. (B) The mechanical properties of the vessel after UV exposure with a water and PEGDA ration of 1:1.7. The insert is the acquired small diameter blood vessel with a internal diameter of 5 mm. The SEM images of different periodic structures formed by double beam interference on the inner surface: 2 μm stripe (C), 4 μm stripe (D), and 4 μm grid (E).

Biomedical Optics EXPRESS

which is of great significance for the construction of artificial blood vessels with multi-level micro-nano structure.

The most effective way to improve the endothelialization process in small-diameter artificial vessels is to process the micro-nano structure on the inner surface of the vessel. When the processed micro-nano structure resembles the structure of the real vessel lining, in vivo tissue cells will more easily infiltrate from the outer side of the vessel and participate directly in the endothelialization process. Here, we use simple and efficient laser double-beam interference to fabricate the micro structure on the anterior surface of small caliber blood vessel, the scheme is shown in Fig. S4. When preparing the micro-nano structure on the inner wall, adjust the optical path so that the focus of the double beam falls on the inner surface of the artificial blood vessel precursor; adjust the rotating speed to 30 rpm, turn on the 355 nm laser (8.1 $mW\mu m^{-2}$), rotate the turntable for one circle, and then close the shutter to complete the preparation of inner wall microstructure. Figure 1(c) and (d) are the SEM images of the processed structures with different period spacing of 2 μm and 4 μm. It can be seen that the structures with different periods are complete and the undulation height is obvious, while Fig. 1(e) is the grid-like structure formed by rotating the processing Table 90 degrees after a single processing.

According to Fig. 1(c)–Fig. 1(e), in addition to the periodic structure formed by interference, the surface of the material also has nanoscale undulating folds after dehydration and drying, which are caused by local uneven dehydration on the surface of the material. Although the degree of undulation varies, the overall undulation pattern is coherent, and no phenomenon such as fracture surface that destroys the function of the material is observed. The surface periodically microscale structure co-existed with the nanoscale structure formed by dehydration and contraction, and the complexity and variability of the structure resembled the complex structure in living organisms, which might further increase the biocompatibility of the synthesized vascular lining. Although the biological toxicity of the photoinitiator Daracure 1173 used in our manuscript has not been carefully studied, with the progress in materials science and biomimetic processing, we believe that there will be many biosafety materials suitable for the preparation of artificial blood vessels and other artificial organs [4849].

2.2. Culture of hcc and huvec on the micro-nano surface

To explore the effect of processed micro-nano structures on the process of vascular endothelialization, we performed adsorption experiments using hcc and huvec on the surface of the blood vessels with micro-nano structures to explore the effect of different cycles and different morphological micro-nano structures on overall cell growth, proliferation, and normal physiological activities. Because alcohol immersion is needed before cell culture, we need to explore the effect of alcohol immersion on the microstructure of artificial blood vessels. As shown in Fig. S5, there is no obvious change in the microstructure of the material surface before and after immersion, which shows that the immersion treatment will not destroy the microstructure formed on the material surface.

The statistics of hepatocellular carcinoma cells cultured was shown in Fig. 2 on the surface of structureless, 4 μm-streaked structural, and grid-like structural PEGDA vessel substrates for 1 h, 24 h, 48 h, and 72 h at different times. The number of cells seeded in the medium was the same, and it can be clearly seen that the morphology of the cells was intact without a large number of dead cells on both structured and unstructured surfaces, thus indicating that the material itself was not toxic to the cells. The value-added rate of cells on the structured surface was significantly higher than that on the unstructured surface, and the tiling effect of cells on the structured surface was also higher than that on the unstructured surface. However, no difference was found between the effect of striated and latticed structures on cell proliferation tiling.

Figure 3 shows the adsorption experiments using huvec on the material surface, where the adsorption of endothelial cells can barely be seen on the structureless surface. As for the structured

Biomedical Optics EXPRESS

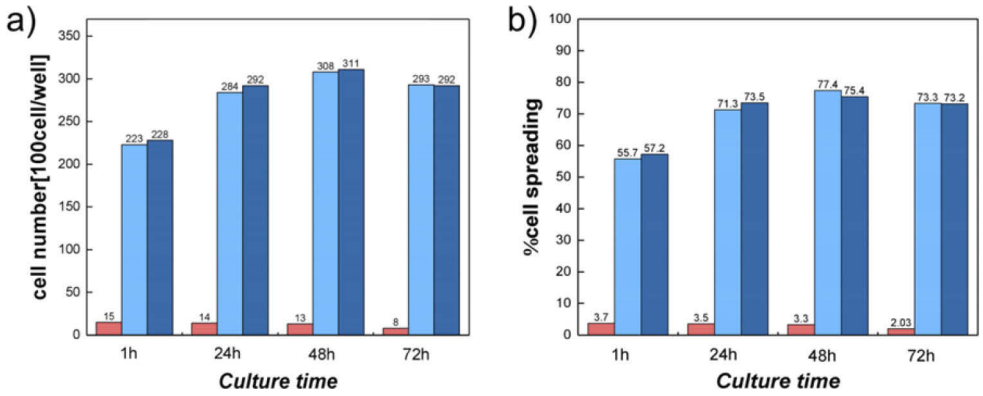

Fig. 2. Statistics of the number of cancer cells (a) and the tiling rate (b)on three different PEGDA surfaces. Red is the unstructured surface, light blue is the striped-structure surface, and dark blue is the grid-structure surface.

surface, the overall cell adsorption was enhanced compared to the structureless one. However, the growth conditions of huvec were significantly harsher than those of hcc, and although the adsorption of cells on the surface of the structure was completed, the cell morphology did not fully unfold. A possible explanation is the fact that the charge on the surface of the material was the same as that of the cells, resulting in the cells not being fully compatible on the surface of the material. Therefore, we used plasma to treat the surface of the material, followed by pH treatment to reach the normal acid-base level of the cells before adsorption culture, and the results were as expected, the endothelial cells not only adsorbed on the surface of the material, but also the cell morphology improved to a great extent compared with the untreated material, as shown in Fig. 4. Fig. S6 shows the large field of view microscopic images of endothelial cells adsorbed on the surface of structured and unstructured materials after plasma treatment, and it can be seen that there is a significant difference in the number of cells on the structured and unstructured surfaces, indicating that materials with microstructures are more likely to adsorb endothelial cells. This indicates that the microstructures processed on the inner surface of the artificial vessels have a significant improvement on the endothelialization process of the vessels, and the modification treatment on the surface can further improve the biocompatibility of the prepared vessels.

To clarify the effect of surface plasma treatment on the cell adsorption, the charge distribution on the surface was measured by electro acoustic pulse method. As shown in Fig. 5, the surface charge of the PEGDA before and after plasma treatment is quite different. After light processing, the surface electrons of PEGDA are trapped by traps in the medium to form space charges. The so-called trap is actually the center of attraction of charge. Any place where the center of positive and negative charge action does not coincide in molecular structure may form traps. For example, impurities, chain breaks, bonds of different atoms can cause the center of positive and negative charge action not to coincide. The charge falling into the trap can no longer move in the electric field due to the electrostatic action of the heteropolar charge, so that the space charge effect will be formed in the medium. Comparing the spatial charge distribution of the three samples, it can be seen that the surface space charge of the PEGDA material is obviously reduced, and the decrease of the space charge makes the cells more easily gathered on the surface of the material. The results show that the processing time has a significant effect on the accumulation of space charge.

Biomedical Optics EXPRESS

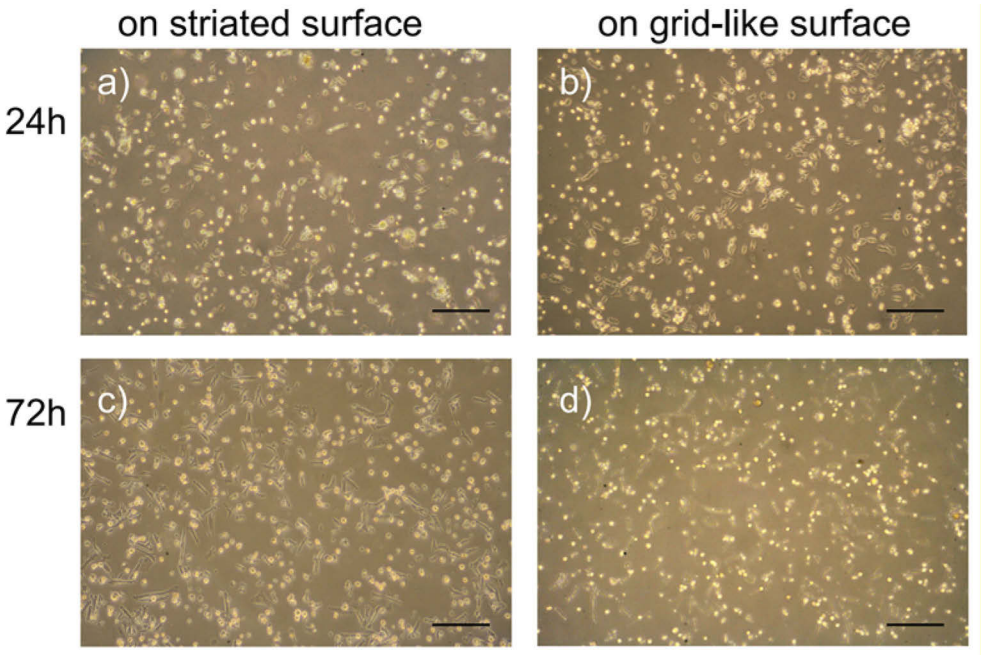

Fig. 3. The cell proliferation and arrangement of huvec on the striated and grid-like surface of 4 μm periodic periods (scale bar: 200 μm).

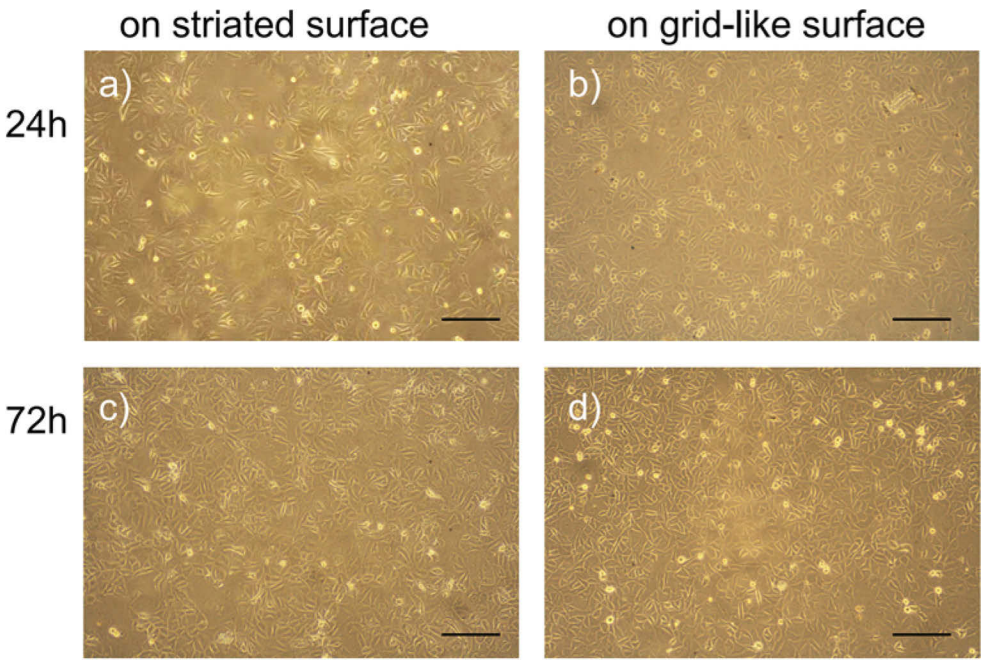

Fig. 4. The cell proliferation and arrangement on the surface of huvec with different culture time after surface plasmon treatment (scale bar: 200 μm).

Biomedical Optics EXPRESS

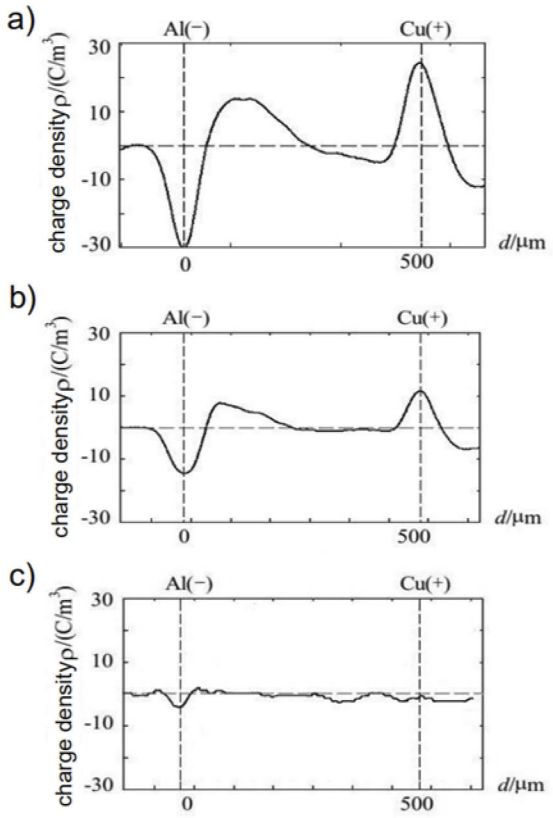

Fig. 5. The charge distribution on the 4 μm striated and grid-like surfaces without plasma surface treatment (a), or with treatment for 1 min (b) and 5 min (c)

3. Conclusions

We designed a new photopolymerization technique for processing small-diameter artificial blood vessels with microstructured inner walls by rotational exposure combined with double-beam interference. The endothelial cell adsorption experiment shows that the vascular can rapidly complete the endothelialization process, which greatly reduces the probability of thrombus blockage in vivo and improves the long-term patency rate. This method provides a new idea for fast and simple preparation of small-diameter blood vessels with high patency and stability.

4. Materials and methods

Materials: Polyethylene glycol diacrylate (PEGDA) and 2-hydroxy-2-methylphenylacetone (Daracure 1173) used in the experiment were purchased from sigma Aldrich.

Preparation of vascular precursors: Firstly, it is necessary to configure the pre-exposure solution under dark room conditions. The PEGDA solution was slowly added into the brown glass bottle, then a certain amount of photoinitiator (Daracure 1173) was added, so that the mass ratio of PEGDA to 1173 is 20:1. Then distilled water was added to it, mix the solution quickly and evenly, keep it away from light for more than 3 hours, wait for the solution mixing process to dissolve into the pre-exposure. The gas in the solution is completely discharged.

Preparation of blood vessels: After the rotary table equipment was built, the pre-exposure solution was moved into the casing spacer layer and the exposure time, exposure distance and exposure speed were adjusted. Then the rotary table was started under the UV lamp equipment

Biomedical Optics EXPRESS

(Shanghai Jiguang lighting equipment factory, Rated Power 350W) for exposure curing. After the exposure was completed (rotating speed 240 rpm, exposure time 5 min, exposure distance 10 cm, 6.5 $mW\mu m^{-2}$), the UV lamp was turned off, the rotary table was stopped, the cannula was removed, and the exposed vascular precursors was slowly removed with forceps. The vascular precursors without inner surface micro-nano structure processing were obtained.

Preparation of small-diameter vessels with internal microstructure: A split-amplitude model optical path was built, so a wider range of interference apertures was obtained in a single pass with a larger range of interference patterns. The beam generated by nanosecond laser (355 nm, Quanta-Ray-150, Spectrum-Physics, USA) was amplitude-separated using a half-transverse, half-transmissive beam splitter, so that the two beams of light with the same frequency and amplitude were basically the same. The two related beams were then focused on the inside of the vessel wall through a reflectors and lens.

After rotational exposure the inner tube was removed, the outer cannula was attached directly to the turntable with the vascular precursor and placed into the optical path as a whole. Before laser double-beam interference processing, the optical power was tested and adjusted using a laser high-power meter to stabilize it at about 300 mW.

A small amount of pre-exposure solution was added to the inside of vascular precursor wall, and the rotary table was started and adjusted to 480 rpm for 3 min. The power density of laser is about 8.1 $mW\mu m^{-2}$ The pre-exposure solution was evenly distributed on the inside of the tube wall at high rotation speed, and then the rotation speed was adjusted to 30 rpm, which was intermittent at low rotation speed due to the periodicity of the square wave. This ensures that the laser interferes with the surface for a long time, allowing the material to be fully cured.

Adsorption experiment of endothelial cells on the inner side of the tube wall: The artificial blood vessel with microstructure on the inner surface prepared by rotary exposure was cut into blocks that could be put into a 6-well plate and put into 75% medical grade alcohol for 6 hours of immersion soaking, and then immersed in saline (0.9%) for 24 hours. The medium and cells corresponding to the serum need to be placed at room temperature (25-27°C) half an hour before use, close to human body temperature before use. The culture medium was dropped onto the new 6-well plate at 800 uL per well, and serum proportionally was added. The vascular block structure was put into the 6-well plate, and the culture medium with cells was added. The culture was incubated for 1 day and then observed.

Funding. National Natural Science Foundation of China (62075081); Natural Science Foundation of Heilongjiang Province (LH2021E001).

Acknowledgements. This work was supported by the Natural Science Foundation of China under Grant #62075081 and Natural Science Foundation of Heilongjiang Province, No. LH2021E001.

Disclosures. The authors declare that there are no conflicts of interest.

Data availability. Data underlying the results presented in this paper are not publicly available at this time but may be obtained from the authors upon reasonable request.

Supplemental document. See Supplement 1 for supporting content.

References

1. T. Misaki, A. Fukunaga, and K. Nakano, "Dental caries status is associated with arteriosclerosis in patients on hemodialysis," Clin. Exp. Nephrol. **25**(1), 87–93 (2021).
2. H. B. Liu, H. X. Zhou, H. M. Lan, T. Y. Liu, X. L. Liu, and H. J. Yu, "3D printing of artificial blood vessel: study on multi-parameter optimization design for vascular molding effect in alginate and gelatin," Micromachines **9**(1), 10 (2017).
3. R. Y. Kannan, H. J. Salacinski, P. E. Butler, G. Hamilton, and A. M. Seifalian, "Current status of prosthetic bypass grafts: A review," J. Biomed. Mater. Res., Part B **74B**(1), 570–581 (2005).
4. P. L. Wu, N. Nakamura, H. Morita, K. Nam, T. Fujisato, T. Kimura, and A. Kishida, "A hybrid small-diameter tube fabricated from decellularized aortic intima-media and electrospun fiber for artificial small-diameter blood vessel," J. Biomed. Mater. Res., Part A **107**(5), 1064–1070 (2019).
5. T. W. Chuang and K. S. Masters, "Regulation of polyurethane hemocompatibility and endothelialization by tethered hyaluronic acid oligosaccharides," Biomaterials **30**(29), 5341–5351 (2009).

Biomedical Optics EXPRESS

6. V. Kappings, C. Grun, D. Ivannikov, I. Hebeiss, S. Kattge, I. Wendland, B. E. Rapp, M. Hettel, O. Deutschmann, and U. Schepers, "vasQchip: a novel microfluidic, artificial blood vessel scaffold for vascularized 3D tissues," Adv. Mater. Technol. **3**(4), 1700246 (2018).`
7. A. de Mel, C. Bolvin, M. Edirisinghe, G. Hamilton, and A. M. Seifalian, "Development of cardiovascular bypass grafts: endothelialization and applications of nanotechnology," Expert Rev. Cardiovasc. Ther. **6**(9), 1259–1277 (2008).
8. D. C. Miller, T. J. Webster, and K. M. Haberstroh, "Technological advances in nanoscale biomaterials: the future of synthetic vascular graft design," Expert Rev. Med. Devices **1**(2), 259–268 (2004).
9. H. J. Kong and D. J. Mooney, "Microenvironmental regulation of biomacromolecular therapies," Nat. Rev. Drug Discovery **6**(6), 455–463 (2007).
10. S. Esmaeili, M. Shahali, A. Kordjamshidi, Z. Torkpoor, F. Namdari, S. Saber-Samandari, M. G. Nejad, and A. Khandan, "An artificial blood vessel fabricated by 3D printing for pharmaceutical application," Nanomed. J. **6**(3), 183–194 (2019).
11. X. Y. Wang, Y. Pei, M. Xie, Z. H. Jin, Y. S. Xiao, Y. Wang, L. N. Zhang, Y. Li, and W. H. Huang, "An artificial blood vessel implanted three-dimensional microsystem for modeling transvascular migration of tumor cells," Lab Chip **15**(4), 1178–1187 (2015).
12. T. L. Sun, H. Tan, D. Han, Q. Fu, and L. Jiang, "No platelet can adhere - Largely improved blood compatibility on nanostructured superhydrophobic surfaces," Small **1**(10), 959–963 (2005).
13. D.-D. Han, Y.-L. Zhang, Y. Liu, Y.-Q. Liu, H.-B. Jiang, B. Han, X.-Y. Fu, H. Ding, H.-L. Xu, and H.-B. Sun, "Bioinspired graphene actuators prepared by unilateral UV irradiation of graphene oxide papers," Adv. Funct. Mater. **25**(28), 4548–4557 (2015).
14. Z.-C. Ma, Y.-L. Zhang, B. Han, X.-Y. Hu, C.-H. Li, Q.-D. Chen, and H.-B. Sun, "Femtosecond laser programmed artificial musculoskeletal systems," Nat. Commun. **11**(1), 4536 (2020).
15. F. Banche-Niclot, G. Montalbano, S. Fiorilli, and C. Vitale-Brovarone, "PEG-coated large mesoporous silicas as smart platform for protein delivery and their use in a collagen-based formulation for 3D printing," Int. J. Mol. Sci. **22**(4), 1718 (2021).
16. J. Xu, X. Yan, X. Ge, M. Zhang, X. Dang, Y. Yang, F. Xu, Y. Luo, and G. Li, "Novel multi-stimuli responsive functionalized PEG-based co-delivery nanovehicles toward sustainable treatments of multidrug resistant tumor," J. Mater. Chem. B **9**(5), 1297–1314 (2021).
17. M. Cheng, L. Zhang, and F. Shi, "Design of functionally cooperating systems and application towards self-propulsive mini-generators," Mater. Chem. Front. **5**(1), 129–150 (2021).
18. M. Cheng and F. Shi, "Precise macroscopic supramolecular assemblies: strategies and applications," Chem. - Eur. J. **26**(68), 15763–15778 (2020).
19. D. Trucco, L. Vannozzi, E. Teblum, M. Telkhozhayeva, G. D. Nessim, S. Affatato, H. Al-Haddad, G. Lisignoli, and L. Ricotti, "Graphene oxide-doped gellan gum-PEGDA bilayered hydrogel mimicking the mechanical and lubrication properties of articular cartilage," Adv. Healthcare Mater. **10**(7), 2001434 (2021).
20. D. Sun, W. Liu, A. Tang, F. Guo, and W. Xie, "A new PEGDA/CNF aerogel-wet hydrogel scaffold fabricated by a two-step method," Soft Matter **15**(40), 8092–8101 (2019).
21. Q. Zhang, Y. Sun, C. He, F. Shi, and M. Cheng, "Fabrication of 3D ordered structures with multiple materials via macroscopic supramolecular assembly," Adv. Sci. **7**(23), 2002025 (2020).
22. F. Ullah, N. Deng, and F. Qiu, "Recent progress in electro-optic polymer for ultra-fast communication," PhotoniX **2**(1), 13 (2021).
23. C. Nam, J. Yoon, S. A. Ryu, C.-H. Choi, and H. Lee, "Water and oil insoluble PEGDA-based microcapsule: biocompatible and multicomponent encapsulation," ACS Appl. Mater. Interfaces **10**(47), 40366–40371 (2018).
24. Y.-L. Sun, W.-F. Dong, R.-Z. Yang, X. Meng, L. Zhang, Q.-D. Chen, and H.-B. Sun, "Dynamically tunable protein microlenses," Angew. Chem. Int. Ed. **51**(7), 1558–1562 (2012).
25. E. Girard, G. Chagnon, A. Moreau-Gaudry, C. Letoublon, D. Favier, S. Dejean, B. Trilling, and B. Nottelet, "Evaluation of a biodegradablePLA-PEG-PLAinternal biliary stent for liver transplantation: in vitro degradation and mechanical properties," J. Biomed. Mater. Res., Part B **109**(3), 410–419 (2021).
26. O. Kulce, D. Mengu, Y. Rivenson, and A. Ozcan, "All-optical information-processing capacity of diffractive surfaces," Light: Sci. Appl. **10**(1), 25 (2021).
27. D. Peng, Z. Huang, Y. Liu, Y. Chen, F. Wang, S. A. Ponomarenko, and Y. Cai, "Optical coherence encryption with structured random light," PhotoniX **2**(1), 6 (2021).
28. S. Juodkazis, "Laser polymerized photonic wire bonds approach 1 Tbit/s data rates," Light: Sci. Appl. **9**(1), 72 (2020).
29. H.-B. Jiang, Y.-L. Zhang, D.-D. Han, H. Xia, J. Feng, Q.-D. Chen, Z.-R. Hong, and H.-B. Sun, "Bioinspired fabrication of superhydrophobic graphene films by two-beam laser interference," Adv. Funct. Mater. **24**(29), 4595–4602 (2014).
30. Z.-Z. Li, L. Wang, H. Fan, Y.-H. Yu, H.-B. Sun, S. Juodkazis, and Q.-D. Chen, "O-FIB: far-field-induced near-field breakdown for direct nanowriting in an atmospheric environment," Light: Sci. Appl. **9**(1), 41 (2020).
31. C. R. Ocier, C. A. Richards, D. A. Bacon-Brown, Q. Ding, R. Kumar, T. J. Garcia, J. van de Groep, J.-H. Song, A. J. Cyphersmith, A. Rhode, A. N. Perry, A. J. Littlefield, J. Zhu, D. Xie, H. Gao, J. F. Messinger, M. L. Brongersma, K. C. Toussaint Jr., L. L. Goddard, and P. V. Braun, "Direct laser writing of volumetric gradient index lenses and waveguides," Light: Sci. Appl. **9**(1), 196 (2020).

Biomedical Optics EXPRESS

32. N. Toropov, G. Cabello, M. P. Serrano, R. R. Gutha, M. Rafti, and F. Vollmer, "Review of biosensing with whispering-gallery mode lasers," Light: Sci. Appl. **10**(1), 42 (2021).
33. M.-D. Qian, Y.-L. Sun, Z.-Y. Hu, X.-F. Fang, J.-L. Zhu, X. Fan, Q. Liao, C.-F. Wu, and H.-B. Sun, "Fluorescent chemosensors based on "dually smart" optical micro/nano-waveguides lithographically fabricated with AIE composite resins," Mater. Horiz. **7**(7), 1782–1789 (2020).
34. S. Masui, Y. Torii, M. Michihata, K. Takamasu, and S. Takahashi, "Fabrication of nano/micro dual-periodic structures by multi-beam evanescent wave interference lithography using spatial beats," Opt. Express **27**(22), 31522–31531 (2019).
35. H. X. Xu, G. W. Hu, Y. Li, L. Han, J. L. Zhao, Y. M. Sun, F. Yuan, G. M. Wang, Z. H. Jiang, X. H. Ling, T. J. Cui, and C. W. Qiu, "Interference-assisted kaleidoscopic meta-plexer for arbitrary spin-wavefront manipulation," Light: Sci. Appl. **8**(1), 3 (2019).
36. Y.-G. Bi, J. Feng, Y.-F. Li, X.-L. Zhang, Y.-F. Liu, Y. Jin, and H.-B. Sun, "Broadband light extraction from white organic light-emitting devices by employing corrugated metallic electrodes with dual periodicity," Adv. Mater. **25**(48), 6969–6974 (2013).
37. Y. Jin, J. Feng, X.-L. Zhang, Y.-G. Bi, Y. Bai, L. Chen, T. Lan, Y.-F. Liu, Q.-D. Chen, and H.-B. Sun, "Solving efficiency-stability tradeoff in top-emitting organic light-emitting devices by employing periodically corrugated metallic cathode," Adv. Mater. **24**(9), 1187–1191 (2012).
38. C. He, M. Steger, and A. Gillner, "High-efficiency nanostructuring using multi-beam interference by consecutively deposited ultrashort laser pulses on tool steel," J. Laser Micro/Nanoeng. **13**(1), 1–5 (2018).
39. C. He, K. Vannahme, and A. Gillner, "High-efficiency sub-micrometer multi-beam interference structuring for large-scale surface using ultrashort laser pulses," J. Laser Micro/Nanoeng. **14**(1), 95–99 (2019).
40. Z. Zhang, L. Dong, Y. Ding, L. Li, Z. Weng, and Z. Wang, "Micro and nano dual-scale structures fabricated by amplitude modulation in multi-beam laser interference lithography," Opt. Express **25**(23), 29135–29142 (2017).
41. D. Nakamura, T. Simogaki, K. Okazaki, M. Higashihata, and T. Okada, "Growth control of ZnO nano-crystals by multi-beam interference patterning," J. Laser Micro/Nanoeng. **8**(3), 206–209 (2013).
42. M. I. Abid, L. Wang, Q.-D. Chen, X.-W. Wang, S. Juodkazis, and H.-B. Sun, "Angle-multiplexed optical printing of biomimetic hierarchical 3D textures," Laser Photonics Rev. **11**(2), 1600187 (2017).
43. Y. Kawamoto, A. Nakao, Y. Ito, N. Wada, and M. Kaibara, "Endothelial cells on plasma-treated segmented-polyurethane: adhesion strength, antithrombogenicity and cultivation in tubes," J. Mater. Sci.: Mater. Med. **8**(9), 551–557 (1997).
44. E. H. Cho, Y. I. Yang, C. W. Mun, and J. K. Kim, "Tissue-engineered semi-microporous segmented polyetherurethane vascular prostheses," J. Biomater. Sci., Polym. Ed. **16**(6), 775–790 (2005).
45. C. Y. Wang, C. L. Lin, R. Ming, X. X. Li, P. Jonkheijm, M. J. Cheng, and F. Shi, "Macroscopic supramolecular assembly strategy to construct 3d biocompatible microenvironments with site-selective cell adhesion," ACS Appl. Mater. Interfaces **13**(24), 28774–28781 (2021).
46. M. J. Cheng, Y. Wang, L. L. Yu, H. J. Su, W. D. Han, Z. F. Lin, J. S. Li, H. J. Hao, C. Tong, X. L. Li, and F. Shi, "Macroscopic supramolecular assembly to fabricate 3D ordered structures: towards potential tissue scaffolds with targeted modification," Adv. Funct. Mater. **25**(44), 6851–6857 (2015).
47. S. Juodkazis, "Writing 3D patterns of microvessels," Int. J. Nanomed. **7**(2012), 3701–3702 (2012).
48. S. Rekstyte, M. Malinauskas, and S. Juodkazis, "Three-dimensional laser micro-sculpturing of silicone: towards bio-compatible scaffolds," Opt. Express **21**(14), 17028–17041 (2013).
49. S. Castelletto, J. Maksimovic, T. Katkus, T. Ohshima, B. C. Johnson, and S. Juodkazis, "Color centers enabled by direct femto-second laser writing in wide bandgap semiconductors," Nanomaterials **11**(1), 72 (2020).